

Band broadening in gel electrophoresis of DNA: Measurements of longitudinal and transverse dispersion coefficients

L. Meistermann and B. Tinland

Institut Charles Sadron, Centre National de la Recherche Scientifique, 6 rue Boussingault, 67083 Strasbourg, France

(Received 8 April 1998; revised manuscript received 15 June 1998)

The experimental determination of the band broadening effect during constant gel electrophoresis of linear DNA has been carried out using the fluorescence recovery after photobleaching technique. The dependence of dispersion coefficients parallel (D_x) and perpendicular (D_y) to the field direction with the electric field and DNA molecular length is presented. The variation of both coefficients can be represented on master curves. Finally, values of the ratio D_x/D_y have been found to be in good agreement with the recent development of the biased reptation model with fluctuations. [S1063-651X(98)01410-X]

PACS number(s): 87.15.-v, 83.20.Fk, 83.10.Nn, 82.45.+z

I. INTRODUCTION

We consider the dynamics of linear DNA molecules undergoing constant field gel electrophoresis. Mobility is the most frequently measured quantity in electrophoresis experiments since its field dependence reduces its molecular size dependence, limiting the separation of DNA [1–3]. Another factor altering DNA separability is the band broadening that reduces the band resolution of the separation, leading in some case to band disappearance [4].

The theoretical models describing the dynamics of DNA during electrophoresis consider the reptation mechanism which assumes that a molecule of radius of gyration R_g greater than the pore size a of the gel can be modeled as a flexible chain constructed of N blobs of size a . The chain is constrained to move in a virtual tube of length L created by the gel fibers. The main models used to describe mechanisms of gel electrophoresis at low electric fields are the biased reptation model (BRM) [5–7] and the biased reptation model with fluctuations (BRF) [8–10]. At very high fields, violations of the model hypothesis such as loop formation (or hernia) and large fluctuations of the tube length can occur, leading to instability of the models. In the BRM, the drift of the chain is biased in the field direction and the leading blob induces the orientation of the whole chain. The BRF takes into account weak fluctuations of the tube length by assuming that the n -end blobs are continuously protruding and retracting and that their mean orientation can be calculated as that of a tethered chain, with a number n decreasing with the field, as a result of competition between Rouse-type fluctuations and drift.

Many features can influence band broadening, such as Brownian diffusion, inhomogeneities in the gel or in the electric field, pH gradient, interactions between DNA due to an overloading well in slab gel, or thermal fluctuations in the molecular conformations leading to a distribution of the mobilities. The band broadening effect is quantified by the measure of the dispersion coefficients D_x and D_y , parallel and perpendicular to the field direction, respectively. The presence of gel prevents band broadening due to convection. Our experimental conditions (low fields, short experiments, large excess of buffer, and DNA concentration below the overlap

concentration) minimize other sources. This means that the factors that are mainly responsible for band broadening are gel inhomogeneities and the distribution of the chain conformations, Brownian diffusion being significant only at very low electric fields. Therefore, we measured here, through the dispersion coefficients, the best resolution achievable in this kind of medium.

Practically, it is important to determine D_x , which reflects the resolution in the field direction; the knowledge of D_y in the direction perpendicular to the field is also essential because it will limit the density of lanes one can use on a gel and it will affect the resolution between bands in two-dimensional electrophoresis. Furthermore, both dispersion coefficients contribute to the blurring of the bands with time, leading finally to their disappearance.

A recent paper reports the D_x dependence on the field strength, the molecular length, and the average pore size. Its behavior is quite well described by the BRF, independently of the system studied [11]. We have shown that measurements of D_x and D_y are possible by combining an electrophoretic cell with a fluorescence recovery after photobleaching (FRAP) technique [12]. This paper was focused on the analysis of the FRAP signal as a function of the scattering vector q and concluded that there is a q domain where quantitative values of D_x and D_y can be extracted from the experimental signal.

In this work we will show more systematic investigations of the lateral dispersion coefficient D_y of differing double stranded DNA molecules in several agarose gels and compare them to the results obtained on D_x . Theoretical expressions of D_y were initially given by Adolf [13] and later by Slater *et al.* [7], within the BRM. Recently, Semenov and Joanny [14] predicted, using the BRF, that in the regime where fluctuations of the tube length are taken into account, the ratio D_x/D_y should be constant.

II. MATERIALS AND METHODS

A. DNA

Samples of lengths of 5721 and 10 900 base pairs (bp) are prepared from commercial corresponding plasmids by linearization and after cutting the native DNA by the specific en-

zyme. We use also standard phage λ DNA (48 500 bp) from Biolabs and T2 DNA (164 000 bp) from Sigma. The DNA solutions are diluted and mixed with a solution of YOYOTM fluorophore (Oxazole Yellow homodimer) from Molecular Probe (1 dye for 150 bp). The low staining level keeps the dynamic behavior of the original chain. The electrophoretic cell used and the sample preparation are similar to previous work [11]. Our cell is half filled with gel, and after casting of the DNA/agarose mixture in the well, filled up with buffer. This ensures a constant pH during the experiments. Since the DNA migrates over a few micrometers (this is an advantage of the FRAP setup compared to migration in macroscopic slab gels) experiments are short (1–30 min in the range of field 0–5 V/cm). Consequently, the temperature rise is around 0.1 °C.

B. The FRAP setup

Measurements were carried out by a fringe pattern fluorescence bleaching technique similar to the one described by Davoust *et al.* [15]. The light beam of an étalon stabilized monomode argon laser ($\lambda = 488$ nm) was split and the two beams were crossed in the electrophoretic cell, providing illumination in an interference fringe pattern. The fringe spacing $i = 2\pi/q$, set by the crossing angle θ ranges from 3 to 60 μm defining the diffusion distance, where the scattering vector q is equal to $(4\pi/\lambda)\sin(\theta/2)$. All the measurements were done in the Guinier regime ($qR_g \ll 1$), ensuring that the size of the molecules is much lower than the fringe spacing. Fluorescence bleaching of the labeled polymers in the illuminated fringes was obtained by producing a 1-s full intensity bleach pulse, thus creating a fringe pattern of concentration of fluorescent molecules identical to the laser interference fringe pattern. The amplitude of the fringe pattern of concentration of fluorescent molecules was detected by modulation of the illuminating fringes position using a piezoelectrically driven mirror and lock-in detection of the emerging fluorescence. The experimental signal decays because of the band broadening and spatial drift of the sample pattern.

Without an electric field, in a polymer solution or in a gel, the diffusion of the macromolecules will lead to a monoexponential decay of the fluorescent contrast with a characteristic time τ . The self-diffusion coefficient D_s is given by

$$D_s = \frac{1}{\tau q^2}. \quad (1)$$

When the fringes are perpendicular to the field direction, the fluorescent concentration fringe pattern will move under the field giving oscillations and will vanish due to the band broadening. The resulting FRAP signal is a damped sinusoid (see Fig. 1) and can be fitted with the expression

$$y = A \exp\left(-\frac{t-t_0}{\tau_1}\right) \sin\left(2\pi\frac{t-t_0}{\tau_2}\right) + B. \quad (2)$$

The time τ_1 , which comes from the exponential decay, corresponds, under certain conditions of q [12], to an apparent diffusion coefficient D_x , which should not be confused with the self-diffusion constant D_s measured in the absence

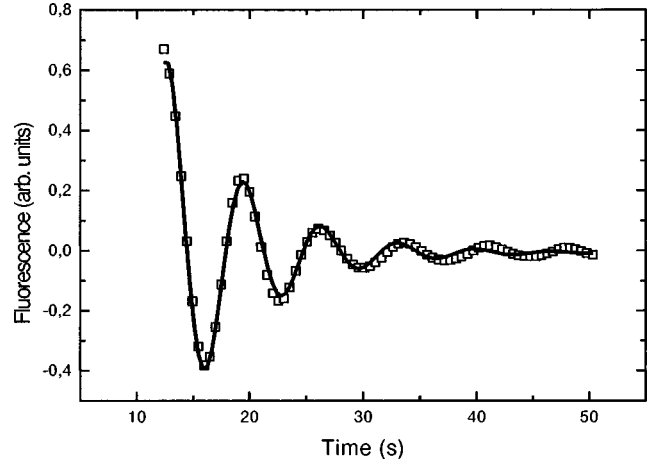


FIG. 1. Typical fit (continuous line) with expression (2) of the damped sinusoidal signal from the FRAP experiment (open squares) of a 5721 bp DNA molecule in a 0.7% agarose gel. The field strength $E = 3$ V/cm, scattering vector $q = 4149$ cm^{-1} .

of an electric field. This decay is mainly related to the distribution of the chain conformations and is the result of the dispersion process. We therefore use the name dispersion coefficient, this coefficient is given by

$$D_x = \frac{1}{\tau_1 q^2}. \quad (3)$$

The time τ_2 is the time to cover the interfringe width i . The corresponding mobility is calculated according to

$$\mu = \frac{i}{E\tau_2}. \quad (4)$$

By rotating the cell 90°, the field direction becomes parallel to the fringes. In this case, there are no longer oscillations and the FRAP signal decays monotonically (see Fig. 2) and can be fitted by a simple monoexponential

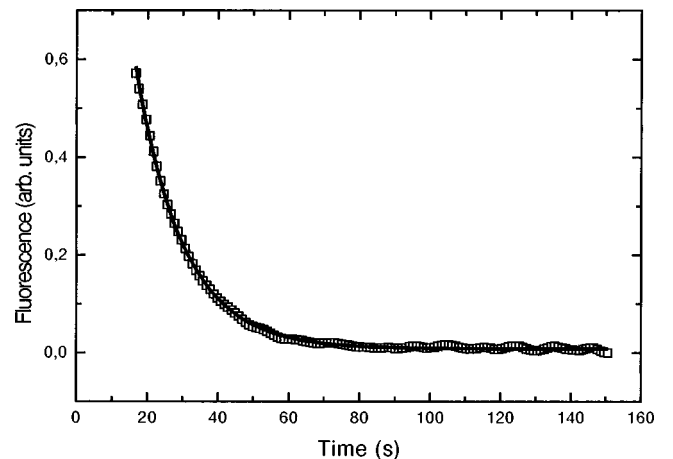


FIG. 2. Monoexponential decay (open squares) obtained when the field direction is parallel to the fringes, fitted with expression (5) (continuous line). Experimental conditions are the same as those of Fig. 1.

$$y = A \exp\left(-\frac{t}{\tau_1'}\right). \quad (5)$$

D_y is given by an expression similar to Eq. (3) using the characteristic time τ_1' .

III. THEORETICAL BACKGROUND

Following the approach suggested by Slater [6], the field dependence of the longitudinal dispersion coefficient has already been given using the arguments of the BRF [9,11]. We will briefly recall these arguments and those from the generalized treatment of the BRF [14] used to establish both D_x and D_y dependences. The DNA molecule is confined in the gel occupying N pores of size a , thus forming a chain of N blobs constrained to move in a virtual tube of length $L = Na$ and diameter a . The electric field is characterized by the dimensionless parameter $\varepsilon = Q Ea / k_b T$ (where Q is the charge per blob). The curvilinear velocity induced by the electric field applied in the x direction is

$$v = \frac{\varepsilon h_x}{N \tau_0}. \quad (6)$$

h_x is the projection of the tube end to end distance along x and τ_0 is the blob relaxation time. The center of mass velocities along the electric field direction x and perpendicular to the electric field direction y are, respectively,

$$\dot{x} = v \frac{h_x}{L} = \frac{\varepsilon a}{\tau_0} \frac{h_x^2}{(Na)^2}, \quad \dot{y} = v \frac{h_y}{L} \quad (7)$$

and the dispersion coefficients in these directions are

$$D_x = \int_0^\infty \langle \dot{x}(0) \dot{x}(t) \rangle dt, \quad (8a)$$

$$D_y = \int_0^\infty \langle \dot{y}(0) \dot{y}(t) \rangle dt. \quad (8b)$$

Given that the characteristic relaxation time of the velocity is the time τ taken by the chain to reptate over the tube length, D_x and D_y can generally be estimated according to the relations

$$D_x \sim \tau (\dot{x})^2, \quad (9a)$$

$$D_y \sim \tau (\dot{y})^2. \quad (9b)$$

At very low field, the tube renewal time is given by the field free reptation theory for the x and y directions [16]:

$$\tau = \frac{L^2}{D_{tube}}, \quad (10)$$

where $D_{tube} = kT / N \zeta$ and ζ is the effective friction coefficient per blob. The chain is Gaussian and thus $\langle h_x^2 \rangle = \langle h_y^2 \rangle = Na^2/3$ using Eqs. (9) we get

$$D_x \sim D_y \sim N^{-2} \varepsilon^0, \quad N < \varepsilon^{-2/3}, \quad \varepsilon \ll 1. \quad (11)$$

When the field increases the tube renewal process is driven by the electric drift, that is, $\tau = L/v$. In the limit $N < N^*$, where $N^* \sim \varepsilon^{-1}$ is the limiting size above which molecules begin to be oriented, the chains are still Gaussian and Eqs. (9) give

$$D_x \sim D_y \sim N^{-1/2} \varepsilon, \quad \varepsilon^{-2/3} < N < N^*, \quad \varepsilon \ll 1. \quad (12)$$

In these two last regimes we have $D_x/D_y = 1$.

For high enough electric fields, the molecules are oriented ($N > N^*$) and the end to end chain projection is fluctuating: $h_x = \eta Na + \delta h_x$, where $\langle \delta h_x^2 \rangle \sim Na^2$ as for a Gaussian chain. The orientation order parameter η is proportional to $\varepsilon^{1/2}$. The corresponding fluctuation of the center of mass velocity is $\delta \dot{x} = 2\varepsilon \eta \delta h_x / N \tau_0$. In this case the longitudinal dispersion coefficient can be expressed as

$$D_x \equiv \int_0^\infty \langle \dot{x}(0) \delta \dot{x}(t) \rangle dt; \quad (13)$$

consequently, Eq. (9a) is replaced by

$$D_x \sim \tau (\delta \dot{x})^2. \quad (14)$$

With Eqs. (14) and (9b) we obtain the scaling arguments

$$D_x \sim D_y \sim N^0 \varepsilon^{3/2}, \quad N > N^*, \quad \varepsilon \ll 1. \quad (15)$$

Assuming that the distribution density function for the end to end projection $\rho(h_x, t)$ obeys the master equation [10]

$$\frac{\partial \rho}{\partial t} = \frac{\partial}{\partial h} \left\{ \frac{\partial}{\partial h} (D^* \rho) - v^* \rho \right\}, \quad (16)$$

where $D^* = v/3$ and $v^*(h_x) \approx v[-h_x/N + (\text{const}/h_x) \varepsilon^{2/3} h_x^{2/3} N^{1/3}] \approx -\beta_x (\delta h_x)$, $\beta_x = \frac{4}{3}(v/N)$, $\delta h_x = h_x - \langle h_x \rangle$, and $\langle h_x \rangle$ is approximately defined by the condition $v^*(\langle h_x \rangle) = 0$. A similar expression can be written for the y component with $v^*(h_y) = -v(h_y/N) = -\beta_y h_y$ considering there is no field orientation in the transverse direction. By rescaling Eq. (16) Semenov and Joanny get

$$\int \langle \delta h_x(0) \delta h_x(t) \rangle dt = C \frac{D^*}{\beta_x^2} \quad (17)$$

and for the y component

$$\int \langle h_y(0) h_y(t) \rangle dt = C \frac{D^*}{\beta_y^2}. \quad (18)$$

C is a universal numerical factor. The ratio of the dispersion coefficients is then

$$D_x/D_y = 4\beta_y^2/\beta_x^2 = 9/4. \quad (19)$$

This value holds for the regime where fluctuations of the chain are considered.

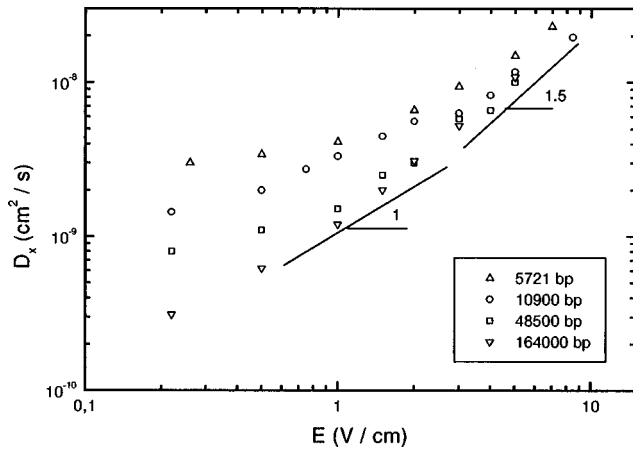


FIG. 3. A log-log plot of the longitudinal dispersion coefficient D_x as a function of the electric field for different DNA molecules in 0.7% agarose gel (lines are guide for the eyes).

IV. RESULTS AND DISCUSSION

A. Scaling laws

We have checked that rotating the cell 90° did not affect the value of the self-diffusion coefficient in the absence of electric field. Systematic measurements of D_x and D_y in several agarose gel concentrations for DNA of different lengths have been carried out. For almost all cases, data error bars are within 10% and smaller than the symbol size. We did not draw them for clarity, because in some regions of the plots data tend to overlap.

For all the possible combinations we observe that the values of the dispersion coefficients in both direction are higher than D_s , they increase with the electric field, and D_x is always larger than D_y (Figs. 3–6). In Figs. 3 and 4 we present respectively the variation of D_x and D_y as a function of the electric field for differing DNA lengths in 0.7% agarose gel. Three regimes are observable. At low fields, for short fragments, dispersion coefficients in both directions are almost independent of E . Their values extrapolated to zero field are consistent with the diffusion coefficient measured without a field. For larger fragments we did not reach sufficiently low

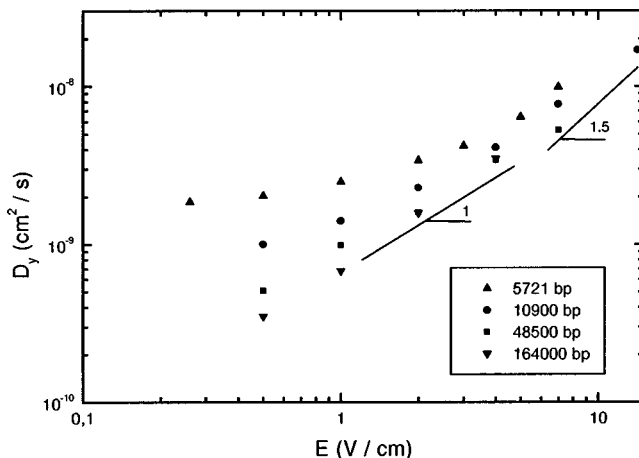


FIG. 4. A log-log plot of the transverse dispersion coefficient D_y as a function of the electric field for different DNA molecules in 0.7% agarose gel (lines are guide for the eyes).

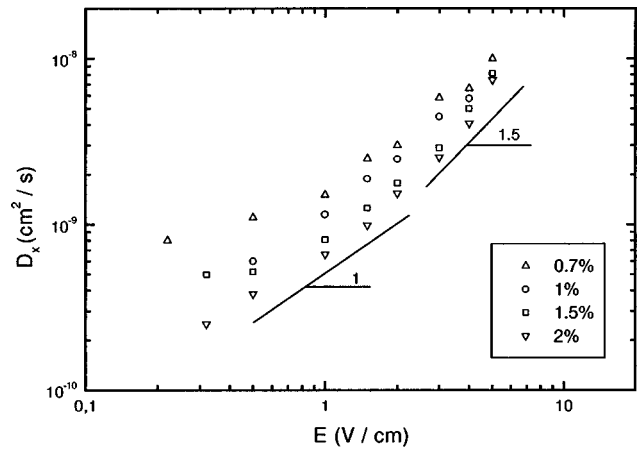


FIG. 5. A log-log plot of D_x versus the electric field for λ DNA in various agarose gel concentrations (lines are guide for the eyes).

fields to observe this behavior. When the field increases, all the curves have a slope close to 1, in good agreement with Eq. (12). Then the slope goes around 1.5 and the dispersion coefficients tend to become independent of N , the number of pores occupied by the chain, as shown by Eq. (15). Figures 5 and 6 show the dependence of D_x and D_y on E for λ DNA in various gel concentrations. The regime where they should become independent of E is not seen for the reason mentioned above for large DNA samples. Increasing the electric strength leads to curves compatible with Eqs. (12) and (15).

B. Master curves

Separation may be achieved in a given range of molecular length using different combinations of the field strength and gel pore size. One may use lower fields with larger pores or larger fields with smaller pores. The pore size is directly linked to the number of pores N occupied by the test chain. To take the above combination into account and neglecting first the a dependence, we chose to represent D_x and D_y over $E^{3/2}$ as a function of EN , where N is calculated from the results of the mobility measurements extrapolated at zero field (see [11]). Then Eqs. (11), (12), and (15) may be rewritten respectively as

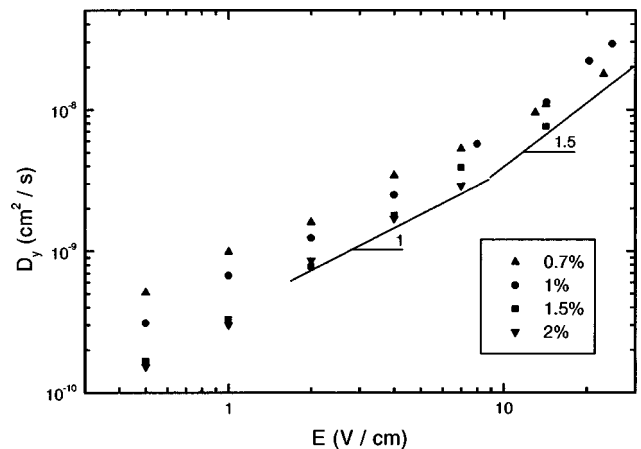


FIG. 6. A log-log plot of D_y versus the electric field for λ DNA in various agarose gel concentrations (lines are guide for the eyes).

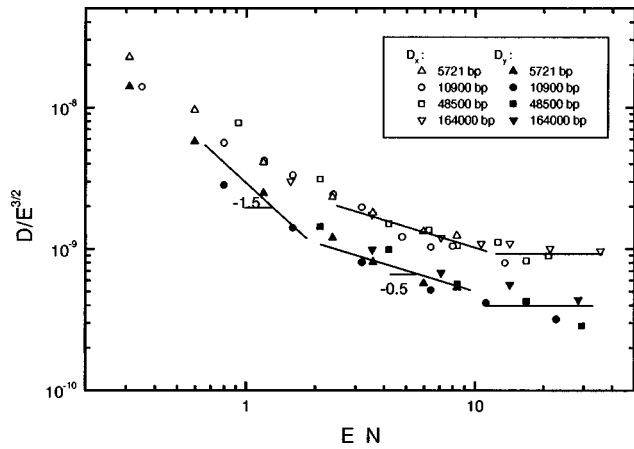


FIG. 7. A log-log plot of $D_x/E^{3/2}$ (open symbols) and $D_y/E^{3/2}$ (filled symbols) as a function of EN for several DNA molecules in agarose gel 0.7%. Lines are forced through the points.

$$D_{x,y}/E^{3/2} \sim (EN)^{-1.5} N^{-0.5}, \quad (20a)$$

$$D_{x,y}/E^{3/2} \sim (EN)^{-0.5}, \quad (20b)$$

$$D_{x,y}/E^{3/2} \sim (EN)^0. \quad (20c)$$

In Figs. 7 and 8 log-log plots of $D_x/E^{3/2}$ and $D_y/E^{3/2}$ as a function of EN are respectively represented for DNA of different sizes in a 0.7% agarose gel and for λ DNA in several gel concentrations. With this representation, the data points describe a master curve giving a general view of the D_x and D_y behavior. The previous three regimes of Figs. 3–6 are again observed in this new representation. The slope -1.5 in the first regime is not truly significant since it depends on the respective weight of E and N . For data points belonging to the second regime we can force a line of slope -0.5 , to guide the eyes, which is compatible with Eq. (20b). The variation of both dispersion coefficients is consistent with Eq. (20c) since there is no more dependence of D_x and D_y over $E^{3/2}$ with EN .

Plotting D_x and D_y over $E^{3/2}$ as a function of EN skips their variation with the average pore size a . To make it explicit, we should have rewritten expressions (11), (12), and

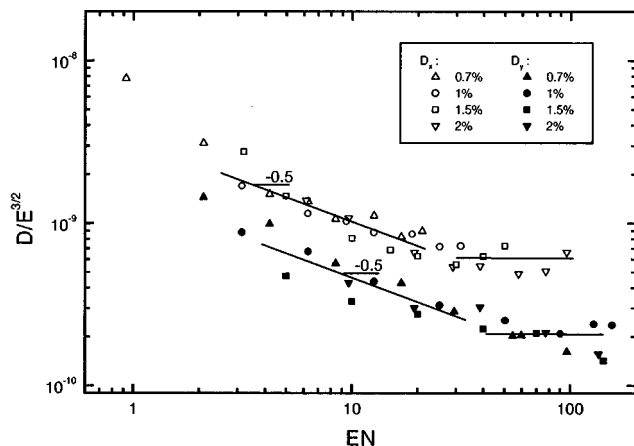


FIG. 8. A log-log plot of $D_x/E^{3/2}$ (open symbols) and $D_y/E^{3/2}$ (filled symbols) as a function of EN for λ DNA in various agarose gel concentrations. Lines are forced through the points.

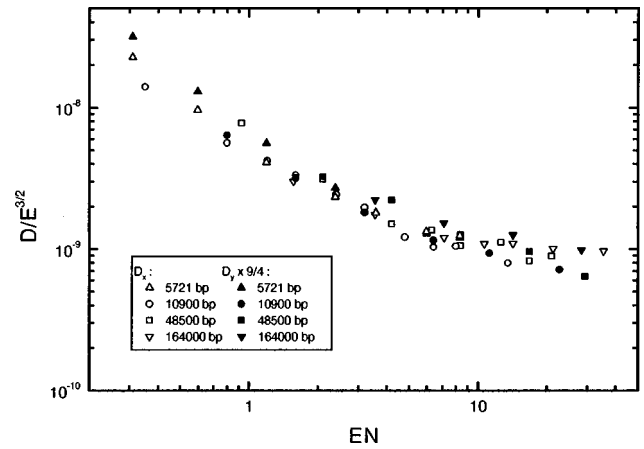


FIG. 9. Same as Fig. 7 with values of D_y multiplied by $9/4$.

(15) with the molecular parameters $N_k = N(a/b)^2$ and $\varepsilon_k = Q_k E b / kT$. This means describing the chain by N_k Kuhn segments of length b , where b is twice the persistence length of the DNA and Q_k represent the charge of a Kuhn segment. This work had already been done and discussed for D_x in another paper [11]. For a constant pore size a (differing DNA lengths in a 0.7% agarose gel), we remark that data of D_x and D_y over $E^{3/2}$ fit nicely on a master curve (Fig. 7). On the other hand, working with various pore sizes (λ DNA in several agarose gel concentrations) gives rise to scattering between the data (Fig. 8), which reflects the a influence; meanwhile, the same trend with EN is still observed. In both cases D_x and D_y follow the same behavior with a and consequently have an equivalent dependence, as described in [11].

C. Quantitative arguments

The dependence of D_x and D_y that is similar to that of EN leads us naturally to examine, through the recent theoretical development of the BRP [14], the value of D_x/D_y . Starting from the lower EN values, D_x and D_y progressively diverge from $D_x = D_y = D_s$, until they reach the third regime, where their ratio becomes constant and close to the predicted value $9/4$ [14]. In fact the model predicts the $9/4$ ratio only in this last regime and D_y should be equal to D_x even in the second regime, since for lower EN fluctuations are not taken into account and $\langle h_x^2 \rangle = \langle h_y^2 \rangle = Na^2/3$. This sharp transition is

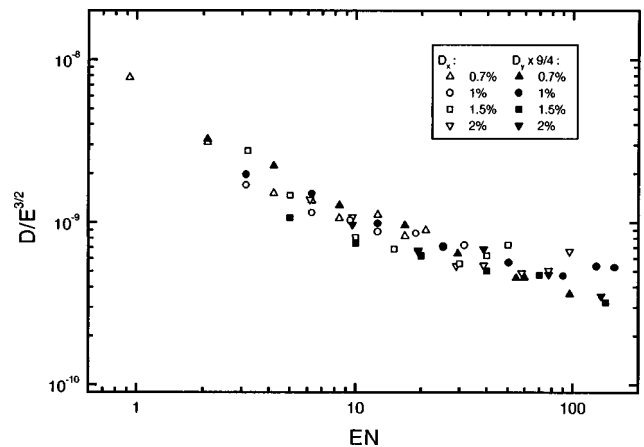


FIG. 10. Same as Fig. 8 with values of D_y multiplied by $9/4$.

not realistic in practice, first probably because molecules start to orient even at low fields leading to anisotropy of the dispersion and because this second domain is a cross over regime. By multiplying D_y values by 9/4, we get values close to D_x (Figs. 9 and 10), demonstrating the good quantitative agreement with Semenov and Joanny's [14] predictions in the regime where dispersion coefficients scale with $E^{3/2}$. As already mentioned, we notice less scattering in Fig. 9 because in this case the pore size a is constant and the N variation is only due to the use of fragments of different lengths.

V. CONCLUSIONS

Measurements of D_y , the transverse dispersion coefficient, have been carried out with an electrophoretic cell coupled to a FRAP setup. As it was shown with D_x , it is possible to draw master curves of D_y as a function of the

separation parameter EN . It is not surprising that the field free diffusion coefficient evolves into D_x under the field influence; the fact that D_y , which is defined in a direction where there is no field applied, presents a behavior similar to the one of D_x concerning the a , E , and N dependence is remarkable and underlines the universal behavior of these quantities. Additionally, the evolution of the ratio D_x/D_y is qualitatively and quantitatively in good agreement with theoretical predictions. These features give weight to the ability of the BRF model to describe the motion of DNA molecules during gel electrophoresis in the low field range defined by $\varepsilon \ll 1$.

ACKNOWLEDGMENTS

The authors are indebted to Professor Souciet's team for kindly supplying the linearized DNA.

-
- [1] H. Hervet and C. Bean, *Biopolymers* **26**, 727 (1985).
 - [2] G. W. Slater *et al.*, *Biopolymers* **27**, 509 (1988).
 - [3] C. Heller, T. Duke, and J. Viovy, *Biopolymers* **34**, 249 (1994).
 - [4] C. Turmel, E. Brassard, G. W. Slater, and J. Noolandi, *Nucleic Acids Res.* **18**, 569 (1990).
 - [5] O. J. Lumpkin, P. Déjardin, and B. H. Zimm, *Biopolymers* **24**, 1573 (1985).
 - [6] G. W. Slater, *Electrophoresis* **14**, 1 (1993).
 - [7] G. W. Slater, P. Mayer, and P. D. Grossman, *Electrophoresis* **16**, 75 (1995).
 - [8] T. A. Duke, A. N. Semenov, and J. L. Viovy, *Phys. Rev. Lett.* **69**, 3260 (1992).
 - [9] T. A. Duke, J. L. Viovy, and A. N. Semenov, *Biopolymers* **34**, 239 (1994).
 - [10] A. N. Semenov, T. A. Duke, and J. L. Viovy, *Phys. Rev. E* **51**, 1520 (1995).
 - [11] B. Tinland, N. Pernodet, and A. Pluen, *Biopolymers* (to be published).
 - [12] B. Tinland, *Electrophoresis* **17**, 1519 (1996).
 - [13] D. Adolf, *Macromolecules* **20**, 116 (1987).
 - [14] A. N. Semenov and J. F. Joanny, *Phys. Rev. E* **55**, 789 (1997).
 - [15] J. Davoust, P. F. Devaux, and L. Leger, *EMBO J.* **1**, 1233 (1982).
 - [16] P. G. de Gennes, *Scaling Concepts in Polymer Physics* (Cornell University Press, Ithaca, 1979).